MORPHOLOGICAL AND FUNCTIONAL CHARACTERIZATION OF THE ATHLETE'S HEART USING ADVANCED ECHOCARDIOGRAPHIC TECHNIQUES

Ph.D. Thesis

Bálint Károly Lakatos MD

Doctoral School of Basic and Translational Medicine
Semmelweis University

Supervisors: Attila Kovács, MD, Ph.D.
Béla Merkely, MD, Ph.D., DSc.

Official reviewers: Zsuzsanna Miklós MD, Ph.D.
Eszter Csajági MD, Ph.D.

Head of the Complex Examination Committee: Tivadar Tulassay MD, D.Sc

Members of the Complex Examination Committee: Péter Andréka MD, Ph.D.
Attila Patócs MD, Ph.D.

Budapest, 2020

1. INTRODUCTION

The adaptation of the cardiovascular system to regular physical exercise has been a subject of research for over a century. In the case of high-intensity regular training, significant changes in cardiac morphology and function is expected, also referred to as the athlete's heart. Beyond the frequency and the nature (dynamic and/or static) of physical exercise, numerous other factors, such as gender, age and racial characteristics may alter this cardiac remodeling. However, in a "typical", mixed-type exercise trained athlete enlargement of the cardiac chambers are expected, while low-normal or even mildly reduced resting functional measures are also not uncommon. This remodeling is considered to be a physiological phenomenon, providing supernormal cardiac function during exercise in order to serve the extreme hemodynamic demands of high-intensity training. Still, several features of the athlete's heart overlap with cardiovascular diseases resulting in unclear distinction of the two entities in the everyday clinical practice.

Several studies have focused on the characterization of these changes, however, despite the large body of literature, data are scarce regarding the longitudinal nature of the exercise-induced cardiac remodeling. Evidence suggests that the morphological and functional characteristics of athlete's heart are highly dynamic and reversible. Still, the in-depth characterization of these temporal changes may be of high interest.

Moreover, the vast majority of studies are focusing on the left ventricle (LV), while the adaptation of the other cardiac chambers may also be highly relevant. Evidence suggest that in the presence of genetic susceptibility, regular training may precipitate certain cardiovascular diseases such as arrhythmogenic right ventricular dysplasia or atrial fibrillation. Therefore, assessment of the right ventricle (RV) and the left atrium (LA), and their physiological remodeling may also have additional clinical value.

Echocardiography is the most frequently used modality to evaluate cardiac morphology and function in athletes. Novel methods of echocardiography, such as speckle-tracking echocardiography (STE) based deformation imaging and three-dimensional (3D)

echocardiography provide incremental information about the exercise-induced changes of the heart. They may gain special importance in the assessment of the RV and LA, in which the more complex geometry and function of these chambers seriously challenges conventional echocardiographic evaluation techniques.

The aim of this present thesis is to explore the role of state-of-the-art echocardiography methods, such as STE and 3D echocardiography in sports cardiology.

2. OBJECTIVES

1. Characterization of the dynamic changes in left ventricular morphology and function induced by exercise training and detraining in a rat model of athlete's heart

Although exercise-induced cardiac hypertrophy has been intensively investigated, the dynamics of its development and regression and subsequent functional changes have not been comprehensively described. Therefore, we aimed to characterize the effects of regular exercise training and detraining on LV morphology and function in a rat model of exercise-induced cardiac hypertrophy.

2. Assessment of the exercise-induced shift in right ventricular contraction pattern

Despite the growing attention concerning RV morphology and function in health and disease, data are limited to the functional adaptation of the RV to intense exercise. Our aim was to characterize the RV mechanical pattern in top-level athletes using 3D echocardiography and also to determine the relationship of RV mechanics to CPET-derived VO2/kg.

3. Unfolding the relationship between left atrial morphology and function and exercise capacity in elite athletes

Data are scarce regarding LA adaptation to regular physical exercise. We aimed to examine LV and also LA morphological and functional remodeling in a large cohort of elite athletes using 3D echocardiography. Beyond the comprehensive assessment of exercise-induced changes in the LA and LV, we also aimed at examining their relationship with CPET-derived exercise capacity.

3. METHODS

3.1 Experimental groups and study design in the rat model of athlete's heart

Young adult, male Wistar rats (n=48, weight=275–325 g) were housed in standard rat cages at constant room temperature (22±2 °C) and humidity with a 12:12-hours light-dark cycle. Rats were fed standard laboratory rodent chow and water ad libitum. After acclimation, twenty-four rats were randomly divided into control (Co, n=12) and exercised groups (Ex, n=12). These rats completed a 12-week-long training and also an 8-week-long detraining period, and during this period, they underwent regular echocardiographic measurements at weeks 0, 4, 8, 12, 14, 16, 18 and 20. At week 20, these animals underwent LV pressure-volume (PV) analysis. Additionally, to obtain hemodynamic data at weeks 0 (baseline) and 12 (end of training period), twelve rats were assigned to groups (Co0, n=6, and Ex0, n=6), and pressure-volume analysis was performed at week 0. Further, twelve rats were used to perform invasive hemodynamic measurements (Co12, n=6, and Ex12, n=6) after completion of the training protocol. Body weight (BW) was measured three times a week during the 20-week-long period. The rats were euthanized after completion of in vivo experiments (PV analysis); the heart was excised, and heart weight (HW) was measured immediately and was indexed to BW values.

3.1.1 Training and detraining protocol

Swim training was performed in a container divided into six lanes filled with tap water (45 cm deep) maintained at 30–32 °C. Rats of exercised groups were exposed to

200 min/day swimming 5 days/week for 12 weeks to induce physiological LV hypertrophy, as described previously.

Thereafter, during the detraining period, animals from both groups remained sedentary for 8 weeks. The duration of the detraining period was chosen according to a pilot study and corresponding literature data.

3.1.2 Echocardiography

Standard two-dimensional long- and short-axis (at the midpapillary level), as well as M-mode images, were acquired using a 13-MHz linear transducer (12L-RS; GE Healthcare, Horten, Norway) connected to a commercially available system (Vivid i; GE Healthcare). Archived recordings were analyzed by a blinded investigator using dedicated software (EchoPac v113; GE Healthcare). On 2D recordings of long-axis and short-axis (at the midpapillary level), LV anterior (AWT) and posterior (PWT) wall thickness in diastole (index: d) and systole (index: s) as well as LV end-diastolic (LVEDD) and end-systolic diameter (LVESD) were measured. All values were averaged over three consecutive cycles. Relative wall thickness (RWT), fractional shortening (FS), LV mass (M) was calculated. To calculate LV mass index (LVMi), we normalized LV mass values to the body weight of the animal. The Teichholz formula was utilized to calculate LV volume values. SV, EF, and CO were determined using standard formulas.

Strain analysis was carried out in accordance with our internal protocol. To quantify GLS and longitudinal systolic strain rate (LSr), three different long-axis recordings from each animal, and three cardiac cycles from each recording were analyzed. To measure global circumferential strain (GCS) and circumferential systolic strain rate (CSr), the same sequence was performed using short-axis loops. After manual contouring of the endocardial border, the software automatically separated the region of interest into six segments and calculated strain and strain rate values, correspondingly. In the case of low tracking fidelity, the contour was further corrected

manually, and the analysis was repeated. Acceptance of a segment to be included in the further analysis was guided by the recommendation of the software.

3.1.3 Hemodynamic measurements – left ventricular pressure-volume analysis

After completion of the training and detraining protocol (at week 20) and in the additional groups (at week 0 and 12), in vivo hemodynamic measurements were performed as described earlier. Shortly, after proper surgical preparation of the animal, a 2-Fr pressure-conductance microcatheter (SPR-838, Millar Instruments, Houston, TX, USA) was inserted into the the LV.

PV loops recorded at different preloads can be used to derive useful indices of LV contractility that are less influenced by loading conditions and cardiac mass. Therefore, LV PV relations were measured by transiently compressing the inferior vena cava (reducing preload) under the diaphragm with a cotton-tipped applicator. The slope of the LV end-systolic PV relationship (ESPVR; according to the parabolic curvilinear model), preload recruitable stroke work (PRSW), and the slope of the dP/dtmax - end-diastolic volume relationship (dP/dtmax-EDV) were calculated as load-independent indices of LV contractility.

All animals were euthanized by exsanguination. Thereafter the heart was quickly removed, and HW was measured.

3.1.4 Histology

The hearts were removed and were fixed in buffered paraformaldehyde solution (4%) and embedded in paraffin. Transverse, transmural, ~5 μm thick slices of the ventricles were cut and placed on adhesive slides.

Hematoxylin and eosin staining was performed to measure cardiomyocyte diameter as a cellular marker of myocardial hypertrophy. In each sample, 100 longitudinally oriented cardiomyocytes from the LV were examined, and the diameters at transnuclear position were defined. The mean value of 100 measurements represented one sample.

The extent of myocardial fibrosis was assessed on picrosirius-stained sections. ImageJ software (National Institutes of Health, Bethesda, MD) was used to identify the picrosirius-red positive area. Three transmural images (magnification 50×) were randomly taken from the free LV wall on each section. The fibrosis area (picrosirius red positive area-to-total area ratio) was determined on each image, and the mean value of three images represents each animal.

3.2 Study groups and methods of the right ventricular and the left atrial assessment in athletes

In our second study, sixty (30 female and 30 male) healthy, young top-level water polo athletes, all of them members of the national teams in the corresponding age group were enrolled). In our third study, inclusion criteria were elite athletes defined by being a member of the national team in the corresponding age group and with a mixed-type exercise regimen (waterpolo [n=113], swimming, [n=11], kayaking [n=14]; n=138). All of the measurements were performed during the in-season competition phase and at least 24 hours after the last athletic training. Detailed medical history and training regime were obtained along with the standard physical examination and 12-lead ECG. Subjects with uncommon echocardiographic and/or ECG features, suboptimal echocardiographic image quality, or athletes who suspended regular training in the last 6 months were excluded. In our second study 40, while in our third study 50 healthy, sedentary volunteers from our existing database (no previous participation in intensive training, <3 hours of exercise/week) with no relevant medical history, no signs or symptoms of cardiovascular disease and normal ECG and echocardiogram served as the control group with similar age and gender distribution.

3.2.1 Echocardiography

ECG gated full-volume 3D datasets reconstructed from 4 or 6 cardiac cycles optimized for the LV, LA, and RV were obtained from apical view with a minimum volume rate of 25 volumes/sec for off-line analysis. Image quality was verified bedside to avoid

“stitching” and “drop-out” artifacts of the 3D data. Further measurements were performed on a separate workstation using dedicated softwares (4D LALV Function and 4D RV Function 2, TomTec Imaging GmbH, Unterschleissheim, Germany). Concerning the LV and the LA, the software detects endocardial surfaces of the chambers, and following manual correction, it traces its motion throughout the cardiac cycle. In the case of the LV, we determined EDVi, ESVi, SVi, and LVMi indexed to BSA, and to characterize global LV function EF and deformation parameters such as GLS and GCS were also assessed. We have also determined RVEDVi and RVESVi to quantify RV 3D morphology, and for the assessment of RV function, we have measured RVSVi, RVEF, and RV free wall longitudinal strain (RVFWLS). Parameters were normalized to body surface area (BSA) calculated by the Mosteller formula.

To examine LA 3D morphology and function, the timing of the late diastolic atrial contraction was confirmed by mitral annular motion to measure LA maximal volume (LAVi), minimal volume (Vmin), and pre A-wave volume (preAV) indexed to BSA. Total emptying volume was defined as LAVi-Vmin. Using these volumetric data, we calculated LA total emptying fraction (EF) as 100*(LAVi-Vmin)/LAVi, LA passive EF as 100*(LAVi-VpreA)/LAVi, and LA active EF as 100*(VpreA-Vmin)/VpreA, as parameters of the LA reservoir, conduit and contractile function, respectively. We have also quantified true conduit volume as LVSVi-(LAVi-Vmin). The software also automatically calculates 3D LAGLS.

3.2.2 Detailed assessment of right ventricular deformation

For the detailed assessment of RV mechanics, the 3D model of the RV was exported frame-by-frame throughout the cardiac cycle for further analysis using our custom made software (Right VentrIcular Separate wall motIon quantificatiON – ReVISION). Briefly, the wall motions of the 3D RV model are decomposed in a vertex-based manner. The volumes of the models accounting for only one motion direction were calculated at each time frame using the signed tetrahedron method. By the decomposition of the model's motion along the three orthogonal, anatomically relevant

axes, volume loss attributable to either longitudinal, radial, or anteroposterior wall motions could be separately quantified. Thus, longitudinal (LEF), radial (REF), and anteroposterior (AEF) ejection fraction and their ratio to global RV EF (LEF/RVEF, REF/RVEF, AEF/RVEF, respectively) could be expressed as a measure of the relative contribution of the given wall motion direction to a global function. 3D RV GLS and GCS was also calculated. In order to examine the regional differences in RV LS and CS, the free wall and the septal surface of the 3D model was separated, and the free wall was divided into three regions (basal, mid and apical parts) by trisection along the vertical axis. The tricuspid and pulmonary annulus were omitted from all analyses.

3.2.3 Cardiopulmonary exercise testing

CPET for peak oxygen uptake quantification was performed on a treadmill using an incremental protocol commencing at a 2 minutes 6 km/h flat race followed by 8 km/h uphill running with an increasing slope of 1.5% every minute until exhaustion. The volume and composition of the expired gases were analyzed breath-by-breath using an automated cardiopulmonary exercise system (Respiratory Ergostik, Geratherm, Bad Kissingen, Germany). Subjects were encouraged to achieve maximal effort, which was confirmed by respiratory exchange ratio, lactate curves by regular fingertip lactate measurements every 2 minutes during the test, and also by reaching the predicted maximal HR and a plateau in oxygen uptake.

3.2.4 Statistical analysis

Data are presented as mean ± SD. In the first study, to compare differences regarding hemodynamic parameters and heart weight data during the 12 weeks of training, two-way analysis of variance (ANOVA) was performed with time and training as factors on data of independent animals in Co0, Ex0, Co12, and Ex12 groups. p values for time x training interaction (piT) were calculated. During the 8-week-long detraining period, two-way analysis of variance (ANOVA) was carried out with time and trained state as factors on data of independent animals in Co12, Ex12, Co, and Ex groups. p values for

time x trained state interaction (piD) were calculated. In the RV study, two-way ANOVA with two factors (gender and sport activity) and their interactions (gender*sport) was used to compare groups, and in the case of significant interaction, Tukey's post-hoc analysis was performed to compare the four study groups. In the LA study, the gender-based matching of the two study groups was confirmed by Chi-square test, and unpaired Student's t-test was used to compare groups. Pearson or Spearman test was applied for correlation analysis as appropriate. Multiple linear regression analysis was applied to find independent predictors that determine VO_2/kg.

4. RESULTS

4.1 Characterization of the dynamic changes in left ventricular morphology and function induced by exercise training and detraining in a rat model of athlete's heart

4.1.1 Heart weight data

HW/BW ratio did not differ between our baseline groups (3.42 ±0.06 g/kg Ex0 vs. 3.39 ± 0.03 g/kg Co0). A marked increase in the HW/BW ratio confirmed cardiac hypertrophy in trained animals (piT= 0.0051; Ex12 vs. Co12: 3.67 ± 0.14 g/kg vs. 2.96 ± 0.16 g/kg), which regressed to control values after the detraining period (piD=0.0012; Ex vs. Co: 2.72 ± 0.04 g/kg vs. 2.73 ± 0.10 g/kg).

4.1.2 Data from LV pressure-volume analysis

Load-independent indices of myocardial contractility (PRSW; ESPVRq and dP/dtmax-EDV) were increased as a result of long-term exercise training. Both conventional and load-independent parameters of systolic function and contractility did not show any difference in week 20, confirming the complete morphological and functional reversibility of exercise-induced alterations.

4.1.3 Echocardiography

While end-diastolic dimensions remained unaltered compared to control animals, end-systolic dimensions significantly decreased in swimming animals, resulting in increased SV and functional measures after 4 weeks of training. RWT clearly increased in the training period, suggesting the appearance of a concentric hypertrophy. Cessation of swim training resulted in a rapid, complete regression of wall thickness, LV mass index, and RWT values: just two weeks after discontinuation of swim training (at week 14), there was no difference between control and exercised groups. This morphological regression was followed by reversion of alterations in cavital dimensions and systolic parameters (FS and EF), which did not differ after 4 weeks of detraining.

4.1.4 Speckle-tracking echocardiography

At week 12, in the trained group, both longitudinal and circumferential strain and strain rate parameters showed a significant increase in systolic function compared to control animals (Figure 1). Consistently with morphological data, an immediate drop in STE-derived parameters could be observed in the trained group after cessation of training. There was no difference between the two groups from week 14 to week 20 (Figure 1).

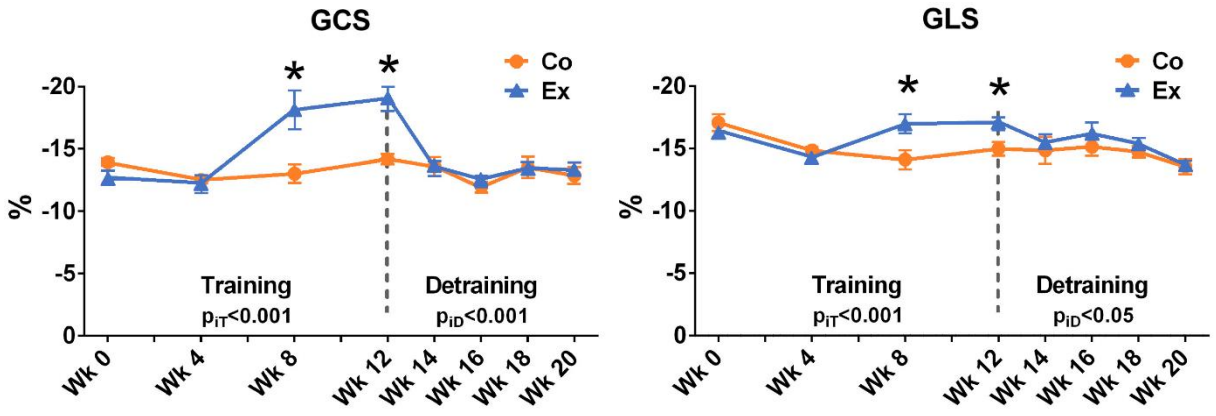

*Figure 1: Speckle-tracking analysis throughout the study period. Results of consecutively measured GCS and GLS during training and detraining. *p < 0.05 Co vs. Ex. piT and piD: interaction value of mixed analysis of variance (ANOVA) during training and detraining, respectively. GLS=global longitudinal strain; GCS=global circumferential strain; Co= control group; Ex=exercise group*

4.1.5 Histology

Increased cardiomyocyte width values were observed in exercised rats compared to control ones after completion of the training program. This exercise-induced alteration showed complete regression after the 8-week long resting period. Picrosirius staining revealed no collagen deposition in the myocardium of exercise-trained rats, that confirms the physiological nature of the observed hypertrophy.

4.2 Assessment of the exercise-induced shift in right ventricular contraction pattern

4.2.1 3D echocardiographic data

As expected, athletes demonstrated increased LV and RV volume indices along with significantly higher LVMi. There was a significant interaction between gender and athletic activity in the case of various LV and RV morphological parameters (LVEDVi, LVESVi, LVSVi, RVEDVi, RVSVi). Post-hoc analysis showed that gender has a significant impact on the degree of geometrical remodeling: while there was no significant difference in ventricular volume indices between the male and female control groups, male athletes demonstrated significantly higher LV and RV volume indices compared to female athletes (all $p<0.01$). LV and also RV EF were significantly lower compared to controls; however, it remained in the normal range in every athlete. Males had significantly lower LV and RV EF, while SVi did not differ between genders. Similarly, LV GLS and GCS were lower in athletes, and also in males.

3D echocardiographic parameters of RV mechanics revealed significant differences between the groups. RV GLS was comparable between the pooled athlete population and controls (-22±5 vs. -23±5 %, $p=0.24$). On the other hand, RV GCS was significantly lower in athletes (-21±4 vs. -26±7 %, $p<0.0001$). This functional shift was even more prominent by examining the relative contribution of longitudinal and radial motion to global function: LEF/RVEF was significantly higher, while REF/RVEF was significantly lower in both athlete groups (Figure 2). REF/RVEF found to be significantly lower in males compared to females.

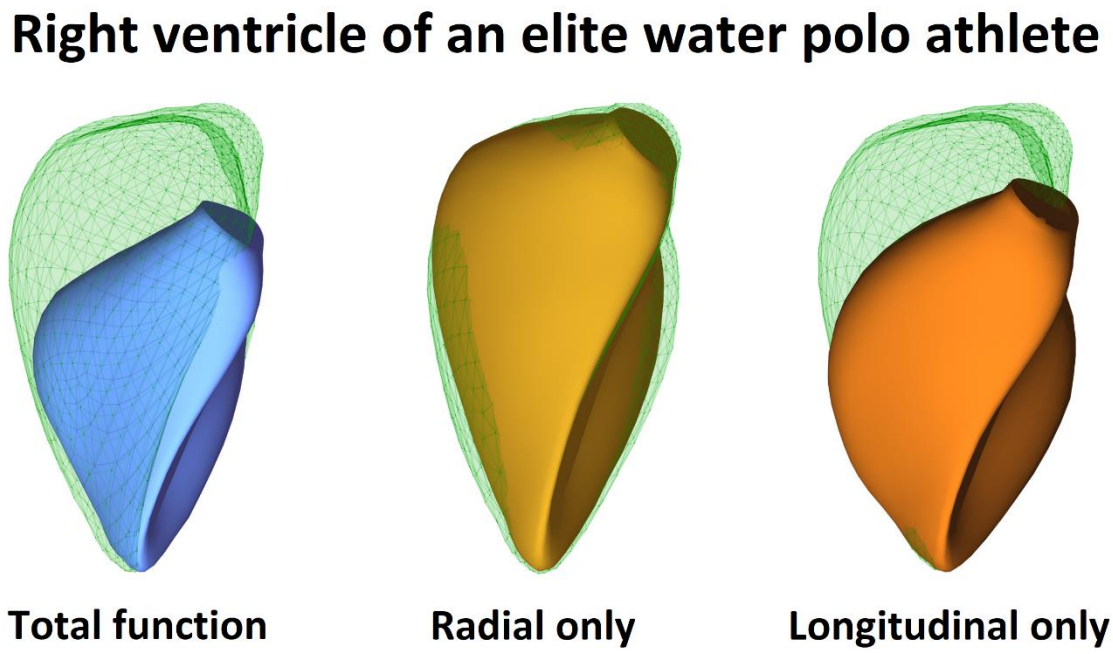

Figure 2.: 3D right ventricular models of an elite athlete. Green mesh represents end-diastolic volume, and the blue surface is the end-systolic volume with all motion directions enabled. By decomposing the motion of the three-dimensional right ventricular model, the different anatomically relevant wall motion directions can be separately quantified. Yellow surface represents the volume loss at end-systole generated by only the radial motion. Orange surface represents the volume loss at end-systole generated by only the longitudinal motion.

Moreover, the degree of this functional shift showed correlation with VO_2/kg (vs. LEF/RVEF: r=0.30; vs. REF/RVEF: r=-0.27, both $p<0.05$). Morphological parameters, such as LVEDVi and RVEDVi, also correlated with CPET-derived VO_2/kg, while no other LV or RV parameter showed a relationship with exercise capacity.

4.3 Unfolding the relationship between left atrial morphology and function and exercise capacity in elite athletes

4.3.1 3D echocardiographic data

Athletes demonstrated significantly higher 3D LV volumes and LVMi compared to controls (Table 1). Functional measures of the LV, such as LV EF, GLS, and GCS, were significantly lower in athletes. Similarly to the morphological changes of the LV, LA dilation was seen in athletes with significantly higher 3D LAVi, Vmin,

preAV, total emptying volume index, and true conduit volume. LAEF and LA active EF was significantly lower in the athlete group (Table 1). LA passive EF did not differ between groups; however, it showed a tendency towards lower values in athletes. Athletes demonstrated lower 3D LAGLS as well. Similarly to the LV, 3D RV volumes were significantly higher in athletes along with lower RVEF; however, RVFWLS was comparable between the athletes and controls (Table 1).

Table 1: 3D echocardiographic data of athlete and control groups

	Athlete (n=138)	Control (n=50)	p value
LVEDVi (mL/m^2)	85.4±12.4	62.0±10.3	**<0.001**
LVMi (g/m^2)	94.9±14.4	68.9±11.7	**<0.001**
LVEF (%)	56.3±4.2	61.6±4.3	**<0.001**
LVGLS (%)	-18.8±1.9	-21.5±1.6	**<0.001**
LVGCS (%)	-27.4±2.9	-29.9±9.0	**<0.01**
LAVi (mL/m^2)	32.0±5.8	26.3±7.7	**<0.001**
LAEF (%)	58.1±6.2	64.2±5.7	**<0.001**
LA active EF (%)	24.1±9.5	32.0±9.6	**<0.001**
LA passive EF (%)	44.6±7.6	46.9±8.0	0.07
LAGLS (%)	32.2±7.3	38.5±7.4	**<0.001**
RVEDVi (ml/m^2)	88.2±13.8	63.5±11.9	**<0.001**
RVEF (%)	54.3±4.8	56.2±6.9	**<0.001**
RVFWLS (%)	-29.1±7.4	-30.6±4.6	0.22

Abbreviations: LVEDVi = left ventricular end-diastolic index; LVMi = left ventricular mass index; LVEF = left ventricular ejection fraction; LVGLS = left ventricular global longitudinal strain; LVGCS = left ventricular global circumferential strain; LAVi: left atrial maximal volume index; LAEF: left atrial total emptying fraction; LA active EF = left atrial active emptying fraction; LA passive EF = left atrial passive emptying fraction; LAGLS: left atrial global longitudinal strain; RVEDVi = right ventricular end-diastolic volume index; RVEF = right ventricular ejection fraction; RVFWLS: right ventricular free wall longitudinal strain

Gender differences were also evaluated. Male athletes had significantly higher 3D LV volume indices and LVMi. On the other hand, LV EF was significantly lower in male athletes, and LV GLS and GCS were also lower compared to female athletes. In contrast with the LV volumetric adaptation, 3D LAVi and Vmin did not differ between genders. Interestingly, however, LA functional differences were present with significantly higher 3D LAEF and LAGLS in females, resulting in a higher total emptying volume index as well. Male athletes demonstrated significantly

higher RV volumes along with lower RVEF compared to females, while RVFWLS did not differ between genders.

We also investigated the correlations between our measured key parameters. 3D LAVi showed weak, but significant positive correlation with age, LVEDVi, LVMi, and RVEDVi. Higher LAEF and LA active EF were weakly associated with higher LV GLS (higher deformation), higher RVEF, and also with higher RVFWLS (better deformation), while LA active EF showed a weak, but significant relationship with LVEF. LA passive EF showed a weak inverse correlation with age. While 2D LA measurements did not show any relationship with VO_2/kg, several 3D LA, LV and RV parameters had weak, but significant correlation with exercise performance: higher LVEDVi, LVMi, LAVi, and RVEDVi were associated with better VO_2/kg, as were lower resting functional parameters, such as LVEF, LVGLS, LAEF, LA passive EF and RVEF. We found no correlation between LA size and LA functional parameters in athletes.

Multiple linear regression models were built to identify independent predictors of VO_2/kg in the athlete group. In our model, 3D LV and LA morphological and functional parameters, such as 3D LAVi, LAEF, LA active EF, LA passive EF, LVEDVi, LVMi, LVEF, LVGLS and LVGCS along with basic demographic and morphometric data (age, gender, BSA) and HR were included in the analysis. According to our results, gender, 3D LAVi, LA passive EF, LVGLS, HR, and BSA were independent predictors of exercise capacity, with an adjusted R^2 value of 0.506 ($p<0.0001$). Male gender was associated with better exercise performance.

5. CONCLUSIONS

In our first study, we have characterized the temporal nature of the development and the regression of exercise-induced cardiac remodeling using conventional echocardiography and STE in a rodent model. We have shown that LV hypertrophy occurs even after 4 weeks of exercise, with a gradual increase in wall thicknesses later on the training period. In parallel with the morphological changes, LV deformation measures increase in a similar manner. Suspension of the training resulted in rapid LV reverse remodeling: both morphological and functional measures were comparable in the study groups 2 weeks following the cessation of the training. We have confirmed enhanced LV contractility of the exercised group and also the deteriorating effects of deconditioning by invasive hemodynamic measurements. Histological examinations also showed the increase and regression of cardiomyocyte width with no concomitant collagen deposition. Our results suggest that STE might be an ideal method to follow-up changes induced by exercise training and detraining.

In our second study, by the 3D echocardiographic assessment of RV mechanical pattern, we have shown that beyond the well-known marked dilation and low-normal resting EF, the RV of the athlete's heart is characterized by an increased relative contribution of the longitudinal and a decreased contribution of radial wall motions at rest. While the morphological changes were less pronounced in females, the RV mechanics did not differ between genders. Moreover, this mechanical pattern shows a correlation with exercise performance measured by CPET. According to these results, this functional shift may represent a novel resting marker of athlete's heart.

Our third study showed significant LV and LA morphological and functional remodeling using 3D echocardiography in a relatively large set of elite athletes. In the face of the lower LV volumes in female athletes compared to males, LA volumes were comparable between genders. Several LV and LA measures showed a significant correlation with exercise capacity; however, 3D LAVmax and LA passive EF were independent predictors of VO2/kg. Our results suggest that athletes' atrial enlargement

and lower resting function do not represent dysfunction, but a physiological aspect of athlete's heart: less contraction in a higher volume chamber can achieve the same stroke volume as a smaller one with more pronounced shortening. Assessment of LA remodeling and phasic function by 3D echocardiography might be an important evaluating step in sports cardiology.

6. BIBLIOGRAPHY OF THE CANDIDATE

6.1 Bibliography related to the present thesis

1. Olah A, Kovacs A, Lux A, Tokodi M, Braun S, **Lakatos BK**, Matyas C, Kellermayer D, Ruppert M, Sayour AA, Barta BA, Merkely B, Radovits T. (2019) Characterization of the dynamic changes in left ventricular morphology and function induced by exercise training and detraining. Int J Cardiol, 277: 178-185. IF: 3.471

2. **Lakatos BK**, Kiss O, Tokodi M, Toser Z, Sydo N, Merkely G, Babity M, Szilagyi M, Komocsin Z, Bognar C, Kovacs A, Merkely B. (2018) Exercise-induced shift in right ventricular contraction pattern: novel marker of athlete's heart? Am J Physiol Heart Circ Physiol.
IF: 4.048

3. **Lakatos BK**, Molnar AA, Kiss O, Sydo N, Tokodi M, Solymossi B, Fabian A, Dohy Z, Vago H, Babity M, Bognar C, Kovacs A, Merkely B. (2020) Relationship between Cardiac Remodeling and Exercise Capacity in Elite Athletes: Incremental Value of Left Atrial Morphology and Function Assessed by Three-Dimensional Echocardiography. J Am Soc Echocardiogr, 33: 101-109 e101.
IF: 6.111

6.2 Bibliography not related to the present thesis

1. **Lakatos B**, Toser Z, Tokodi M, Doronina A, Kosztin A, Muraru D, Badano LP, Kovacs A, Merkely B. (2017) Quantification of the relative contribution of the different right ventricular wall motion components to right ventricular ejection fraction: the ReVISION method. Cardiovasc Ultrasound, 15: 8.
IF: 2.043

2. Matyas C, Kovacs A, Nemeth BT, Olah A, Braun S, Tokodi M, Barta BA, Benke K, Ruppert M, **Lakatos BK**, Merkely B, Radovits T. (2018) Comparison of speckle-tracking echocardiography with invasive hemodynamics for the detection of characteristic cardiac dysfunction in type-1 and type-2 diabetic rat models. Cardiovasc Diabetol, 17: 13.
IF: 5.948

3. **Lakatos BK**, Tokodi M, Assabiny A, Toser Z, Kosztin A, Doronina A, Racz K, Koritsanszky KB, Berzsenyi V, Nemeth E, Sax B, Kovacs A, Merkely B. (2018) Dominance of free wall radial motion in global right ventricular function of heart transplant recipients. Clin Transplant, 32: e13192.
IF: 1.667

4. Molnar AA, Kovacs A, **Lakatos BK**, Polos M, Merkely B. (2018) Sinus of Valsalva aneurysm protruding intramurally into right ventricle: does size really matter? Eur Heart J Cardiovasc Imaging, 19: 234.
IF: 5.260

5. Kovacs A, Molnar AA, Kolossvary M, Szilveszter B, Panajotu A, **Lakatos BK**, Littvay L, Tarnoki AD, Tarnoki DL, Voros S, Jermendy G, Sengupta PP, Merkely B, Maurovich-Horvat P. (2018) Genetically determined pattern of left ventricular function in normal and hypertensive hearts. J Clin Hypertens (Greenwich), 20: 949-958.
IF: 3.402

6. Doronina A, Edes IF, Ujvari A, Kantor Z, **Lakatos BK**, Tokodi M, Sydo N, Kiss O, Abramov A, Kovacs A, Merkely B. (2018) The Female Athlete's Heart: Comparison of Cardiac Changes Induced by Different Types of Exercise Training Using 3D Echocardiography. Biomed Res Int, 2018: 3561962.

IF: 2.197

7. Kovacs A, **Lakatos B**, Nemeth E, Merkely B. (2018) Response to Ivey-Miranda and Farrero-Torres "Is there dominance of free wall radial motion in global right ventricular function in heart transplant recipients or in all heart surgery patients?". Clin Transplant, 32: e13286.

IF: 1.667

8. Kovacs A, **Lakatos B**, Tokodi M, Merkely B. (2019) Right ventricular mechanical pattern in health and disease: beyond longitudinal shortening. Heart Fail Rev, 24: 511-520.

IF: 4.196

9. Csecs I, Czimbalmos C, Toth A, Dohy Z, Suhai IF, Szabo L, Kovacs A, **Lakatos B**, Sydo N, Kheirkhahan M, Peritz D, Kiss O, Merkely B, Vago H. (2020) The impact of sex, age and training on biventricular cardiac adaptation in healthy adult and adolescent athletes: Cardiac magnetic resonance imaging study. Eur J Prev Cardiol, 27: 540-549.

IF: 5.640

10. Tokodi M, Schwertner WR, Kovacs A, Toser Z, Staub L, Sarkany A, **Lakatos BK**, Behon A, Boros AM, Perge P, Kutyifa V, Szeplaki G, Geller L, Merkely B, Kosztin A. (2020) Machine learning-based mortality prediction of patients undergoing cardiac resynchronization therapy: the SEMMELWEIS-CRT score. Eur Heart J.

IF: 24.889

11. Tokodi M, Németh E, **Lakatos BK**, Kispál E, Tősér Z, Staub L, Rácz K, Soltész Á, Szigeti S, Varga T, Gál J, Merkely B, Kovács A. (2020) Right ventricular mechanical pattern in patients undergoing mitral valve surgery: a predictor of post-operative dysfunction? ESC Heart Failure, [Epub ahead of print].

IF: 3.407

12. **Lakatos BK**, Kovacs A (2020) Global Longitudinal Strain in Moderate Aortic Stenosis: A chance to Synthesize It All? Circ Cardiovasc Imaging 2020 Apr;13(4):e010711.

IF: 5.813

13. **Lakatos BK**, Nabeshima Y, Tokodi M, Nagata Y, Toser Z, Otani K, Kitano T, Fabian A, Ujvari A, Boros AM, Merkely B, Kovacs A, Takeuchi M (2020) Importance of non-longitudinal motion components in right ventricular function: 3D echocardiographic study in healthy volunteers J Am Soc Echocardiogr. [in press]
IF: 6.111

14. Ruppert M, **Lakatos BK**, Braun S, Tokodi M, Karime C, Olah A, Sayour AA, Hizoh I, Barta BA, Merkely B, Kovacs A, Radovits T (2020) Longitudinal strain reflects ventriculo-arterial coupling rather than mere contractility in rat models of hemodynamic overload-induced heart failure J Am Soc Echocardiogr. [in press]
IF: 6.111

Hungarian articles:

1. **Lakatos B**, Kovács A, Tokodi M, Doronina A, Merkely B. (2016) A jobb kamrai anatómia és funkció korszerű echokardiográfiás vizsgálata: patológiás és fiziológiás eltérések. Orv Hetil. 157(29):1139-46.
IF: 0.564

2. Ujvári A, Komka Z, Kántor Z, **Lakatos BK**, Tokodi M, Doronina A, Babity M, Bognár C, Kiss O, Merkely B, Kovács A (2018) Kajakos és kenus élsportolók bal és jobb kamrai analízise 3D echokardiográfia segítségével Cardiol Hung 48: 13–19

3. Suhai FI, Sax B, Assabiny A, Király Á, Czimbalmos C, Csécs I, Kovács A, **Lakatos B**, Németh E, Becker D, Szabolcs Z, Hubay M, Merkely B, Vágó Hajnalka (2018) A szív MR-vizsgálat szerepe kevert típusú (humorális és celluláris) kardiális allograft rejekció esetén Cardiol Hung 48: 44–51

4. Fábián A, **Lakatos BK**, Kiss O, Sydó N, Vágó H, Czimbalmos C, Tokodi M, Kántor Z, Bognár C, Major D, Kovács A, Merkely B (2019) A jobb kamrai kontrakciós mintázat változása élsportolókban: háromdimenziós echokardiográfiás vizsgálat Cardiol Hung 49: 17–23